NASA

Technical Memorandum **80566**

HEAO-A2 Observations of the X-Ray Spectra of the Centaurus and A1060 Clusters of Galaxies

R. Mitchell and R. Mushotzky

OCTOBER 1979

National Aeronautics and Space Administration

Goddard Space Flight Center
Greenbelt, Maryland 20771

HEAO-A2 OBSERVATIONS OF THE X-RAY SPECTRA OF THE CENTAURUS AND A1060 CLUSTERS OF GALAXIES

R. Mitchell* and R. Mushotzky**

Laboratory for High Energy Astrophysics
NASA/Goddard Space Flight Center
Greenbelt, Maryland 20771

ABSTRACT

X-ray spectral observations of two nearby low-luminosity clusters of galaxies are presented. For the Centaurus cluster an emission feature at 7.9 keV is detected at about one third of the strength of the 6.7 keV line. This higher energy line represents Kβ emission from highly ionized iron. In addition, it is demonstrated that for neither the Centaurus nor A1060 clusters can an isothermal model with an Fe emission line adequately fit the data. Instead, the simplest models which provide acceptable fits include a second harder component which may be either a second exponential or a power law. The implications of the two component nature of the continuum on the Fe abundance and the X-ray surface brightness distribution are discussed.

Subject headings: galaxies: clusters of - X-rays: sources - X-rays: spectra

* Institute of Astronomy, Cambridge University, England

** NAS/NRC Research Associate

I. INTRODUCTION

The Centaurus and A1060 clusters of galaxies were observed for 7 hours on July 25, 1978 and 6 hours on 6-7 May, 1978 respectively with the A-2 experiment on board the HEAO-1 satellite[+]. Nominal pointing positions were $\alpha\ 12^H\ 46\overset{M}{.}2$, $\delta' = -41^o\ 02'$ and $\alpha = 10^H\ 33\overset{M}{.}5$, $\delta = -27^o\ 01'$ (1950.0 coordinates) with fluctuations of up to $0\overset{o}{.}4$. The data analyzed came from two detectors, referred to as MED and HED3, each having two co-aligned fields of view of $3^o \times 3^o$ and $3^o \times 1\frac{1}{2}^o$ FWHM. For the MED, 49 channels of pulse height data sensitive to the energy range 1.9 - 18 keV were employed; for the HED3, spectral information was collected in 52 channels corresponding to the energy band 3.3 - 67 keV. A full description of the A-2 experiment is given elsewhere (Rothschild et al. 1979).

[+]The A-2 experiment on HEAO-1 is a collaborative effort led by E. Boldt of GSFC and G. Garmire of CIT, with collaborators at GSFC, CIT, JPL and UCB.

The MED is a $\sim$ 800 cm^2 argon counter with a 3 mil. beryllium window while HED 3 is an $\sim$ 800 cm^2 xenon counter with a propane anti-coincidence layer contained within 2, 1 mil. mylar windows.

II. PREVIOUS X-RAY STUDIES OF THE CENTAURUS CLUSTER

X-ray emission from the Centaurus cluster was discovered by the detectors on Uhuru (Gursky et al. 1972). The flux measured, 5.9 Uhuru counts, placed Centaurus at the low end of the X-ray luminosity function for clusters of galaxies, and the emission region was found to be extended with a core radius of $16\overset{!}{.}2\ ^{+7\overset{!}{.}0}_{-5\overset{!}{.}4}$ for an isothermal gas sphere distribution (Kellogg and Murray 1974). Copernicus observations of NGC4696, the giant

elliptical galaxy at the centre of the Centaurus cluster, indicated that this galaxy is itself a source of soft, $\lesssim$ 3 keV, X-ray emission and that there is no pronounced low energy absorption (Mitchell et al. 1975).

Detailed spectral observations of the cluster have been made by the X-ray spectrometers on both Ariel V (using an argon counter) and OSO-8 (using a xenon counter) (Mitchell and Culhane 1977; Mushotzky et al. 1978). Both have observed an FeXXV-XXVI blend at around 6.7 keV, but the best fitting continuum based on an isothermal model which includes a Gaunt factor differs significantly for the two detectors. Ariel 5 derived a best-fit temperature of $3.6 \pm .2$ keV whereas the corresponding value from the OSO-8 data was $5.3 \, ^{+1.1}_{-0.8}$ keV; no significant cut-off was found by either detector. The Uhuru data, although less well resolved in energy, were consistent with an exponential spectrum having a temperature in the range 2.6 - 3.7 keV (Jones and Forman 1978).

III. HEAO-A2 OBSERVATIONS OF CENTAURUS

Data from the small ($1\frac{1}{2}^{o}$ x 3^{o}) and large (3^{o} x 3^{o}) fields of view scalars were combined and deconvolved using various trial spectra. An exponential spectrum which included a temperature-weighted Gaunt factor (Kellogg, Baldwin and Koch 1975) was found to give an unsatisfactory fit, as determined by the χ^2_{min} criterion, to both the MED and HED3 data. This simple model did however reveal several interesting features. First, no significant absorption effect could be measured; second, even in the unconvolved data an excess flux at around 7 keV was apparent; third, the best-fitting temperature to the MED data was significantly lower than that measured by the HED 3. These results suggested that, not only was the 6.7 keV iron lines blend a prominent feature in the data, but also that the continuum was complex.

As a first step towards obtaining an acceptable model a 6.7 keV narrow emission line (with a $\pm$ 0.5 keV energy uncertainty) was included in the trial spectrum. For both detectors the goodness-of-fit improved considerably and the derived temperature values were slightly reduced but remained inconsistent. Best-fit parameter values and the corresponding χ^2_{min} are given in Table 1A. For comparison, the fits to an isothermal model without a line feature are also included.

The major discrepancy between the data and the single continuum and iron line model appears to be excess counts, both at high ($\gtrsim$ 12 keV) energies and at around 8 keV. A second continuum, also an exponential, was therefore added to the model, and once again the fits to both MED and HED3 data were significantly improved. Although hydrogen column density was included as a free parameter for both continua the best-fit parameters were consistent with negligible absorption. Reasonable agreement was obtained between both high and low temperature values derived from the MED and HED 3 data, and the inclusion of the second component was able to account for the high energy excess.

The 6.7 keV Kα iron lines blend represents transitions between the 2 and 1 levels for the FeXXV and FeXXVI states. Other transitions can however also occur and, in particular, for these same ionized states, a second blend of Fe lines, Kβ, exists at around 7.9 keV for the transitions between the 3 and 1 levels. The resultant intensity, although temperature dependent, is less than that of the 6.7 keV feature, but with the energy resolution and high counts available should be discernable.

A second, 7.9 keV line, again with a $\pm$ 0.5 keV uncertainty, was therefore included in the model instead of the second continuum. Resultant χ^2_{min} values were found to be almost identical to those obtained for the 2 continua - 1 line case, so that either a second line or a second continuum

are equally acceptable. Table 1B lists parameter and χ^2_{min} values for fits to these models.

The next stage in the fitting procedure was to determine whether the data could be better represented by including both continua and both lines in the trial model. Once again significant improvements in the resulting χ^2_{min} values were achieved for both detectors by including the extra features, and other considerations also support this 4-component model. First, the MED and HED 3 best-fit values of both high and low temperatures and of line intensities are consistent. Second, the peak emission energies of the lines are all in excellent agreement with theoretical values, redshift effects being negligible for this cluster. Third, the ratio of the fluxes in the 7.9 to 6.7 keV lines is the same for both detectors. Parameters for the 4-component model are given in Table 1C.

Figures 1 and 2 show the fits of various trial models to the MED (Figure 1) and the HED 3 (Figure 2) data, as well as the deconvolved spectra based on the best fit to two exponentials and two lines (Figures 1c and 2c). Figures 1a and 2a are for fits to a single isothermal gas and emission from the 6.7 keV iron lines blend. Figures 1b and 2b show the fits to the 2 exponentials and 2 lines model and also demonstrate the individual contributions from the two continua.

It is important to consider the reality of and the uncertainties in the 4-components used to fit the data. For the simple models the high values of χ^2_{min} mean that since the possibility that such models be correct is negligible, no meaningful error bars can be obtained. In contrast, for the more complex models only certain parameters can reasonably be assigned error bars of the form $\pm \Delta\chi$, where $\Delta\chi$ refers to, for example, a 2σ confidence level. Because 4-components provide a good fit to the

data does not mean that they all must exist. Both the Ariel 5 and OSO-8 data were consistent with a single exponential plus a 6.7 keV line model. With yet further improved resolution and higher counts the situation might be shown to require a more complex solution.

Despite this, there can be little doubt of the reality of the 6.7 keV and 7.9 keV iron line blends, and since their intensities are relatively independent of the forms assumed for the underlying continua and of each other it is possible to derive meaningful limits for these intensities. These are illustrated in Figure 3 in which χ^2 is plotted against line strength for both lines as seen by both detectors. That the plasma is characterized by two distinct temperature regions is less certain however and, even assuming that this is correct, defining confidence contours is complicated because of their dependence upon each other. This is illustrated in Figure 4 in which confidence contours are plotted for the low temperature--high temperature regime for both detectors.

The presence of high ionization emission lines requires the existence of some thermal component. However, since the data negate a single temperature plasma, it is possible that one continuum component arises from non-thermal emission. In order to test this possibility, a power law function was used in the model instead of one of the exponentials. The goodness of fit was acceptable for both the MED nor the HED 3 data, so that it is not yet possible to determine whether or not a non-thermal process contributes significantly to the X-ray spectrum. Again, no significant absorption could be measured. It is perhaps of interest that only the high-temperature continuum could be replaced by a power law if an acceptable fit was to be obtained. For example, if for the MED data the temperature of the exponential function was maintained at $\geq$ 5 keV a χ^2_{min} value of 67, more than twice the value for a low temperature component, was returned. The

parameter values for the best-fit models which include a power law are given in Table 1D. As for the 2-exponential case, the ranges of acceptable values for kT and for α, the power law photon index, are interdependent.

IV. THE CLUSTER A1060

A1060 has the lowest redshift of any cluster in Abell's (1958) catalogue. It is also the lowest-luminosity X-ray cluster yet identified (Ives and Sanford 1976). Although the cluster appears to be a good candidate for the X-ray source, because the flux is so weak the various error boxes so far derived are fairly large. The HEAO-A2 error box which was obtained from scanning-mode data is shown in Figure 5 and thus further strengthen the identification with the cluster. The Ariel 5 and OSO-8 spectrometers both measured a steep spectrum showing little or no absorption for A1060 (Mitchell et al. 1979; Mushotzky et al. 1978). Best-fit temperatures were essentially in agreement, slightly above 3 keV, but no other features could be resolved.

The HEAO-A2 spectral data analysis for A1060 is summarized in Table 2. Although the source is weaker than Centaurus and the statistics are correspondingly worse, the two clusters appear to share several X-ray properties. A single temperature plasma does not provide a good fit to the A1060 data, and the value for the temperature derived from the HED3 (3.83 keV) is higher than that from the MED (3.15 keV). The 6.7 keV iron line is seen at a high significance level in both data sets although the higher energy iron feature cannot be detected. Either a second, high temperature, exponential or a power law function provides an acceptable fit to the data in a two-continuum model. The fits to the data and the corresponding deconvolved spectra are illustrated in Figures 5 and 6.

Because A1060 is a soft, weak X-ray source, the higher energy data are particularly sensitive to systematic errors brought about because of small fluctuations in the background. This is a possible cause of the χ^2_{min} value for the best-fit to the HED 3 data being worse than that for the MED data, an effect also noticable but less pronounced for the Centaurus cluster. This results in several of the higher energy channels registering small negative fluxes which prevent χ^2 from converging to $\sim$1 per degree of freedom for any of the trial spectra employed. Note, however, that this effect is in no way responsible for producing the second continuum since it works in the opposite sense, removing as opposed to adding flux. Also, the high temperature continuum is best observed at intermediate energies (10 - 25 keV) where the statistical significance of the data is far higher. The channels above 25 keV in fact barely affect the results in any way and are only considered for consistency since for stronger and harder sources such as Perseus they measure significant fluxes.

Although for A1060 no line feature was detected at around 7.9 keV we note that the strength of the 6.7 keV line is only about one third of that measured in the Centaurus cluster. If the flux ratio of the 7.9 to 6.7 keV lines is the same for both clusters the higher energy feature would not be expected to be seen to better than about 1σ above the continua.

V. DISCUSSION

A. Fe Abundance

Interpetation of the strength of the Fe lines in terms of an Fe abundance requires a model as to the distribution of the Fe in the two thermal components. In the extremes of all the Fe coming from the low temperature gas one can derive an Fe abundance in that gas of Fe/H $\sim$

5×10^{-5} by taking the ratio of the Fe line to the low kT continuum only. Making the assumption that all the Fe line comes from the high kT material leads to Fe/H $\sim 4.7 \times 10^{-5}$. Clearly these values are both upper limits. If one assigns the Fe line to a "mean" continuum and a "mean" temperature of $\sim$ 4 keV one obtains Fe/H $\sim 2 \times 10^{-5}$. Weighting the contribution to the Fe emission by the ratio of the emission measures of the two components and assuming that they each have equal Fe abundances one derives Fe/H $\sim$ 1.5×10^{-5}. Therefore, there is no evidence for an Fe/H ratio in Centaurus different from that in other clusters (Mushotzky et al. 1978). One can perform similar calculations for A1060 with similar results for the Fe abundance, however the relatively larger contribution of the high kT component to the total emission integral makes the results even more uncertain.

Because of the insensitivity of the ratio of Kα to Kβ over the range of temperatures in these two clusters we can only comment that our limits on this ratio are consistent with theoretical predictions (Raymond and Smith 1977) and provide little additional information as to the origin of the Fe lines.

B. Implications of a Two Temperature Model

All four clusters, having X-ray luminosity less than 3×10^{44} erg s^{-1} and good exposure by the A-2 experiment, show two temperature components. This includes Virgo (Mushotzky et al. 1978) and A2147 (Pravdo et al. 1979).

Assuming the two temperature model one can look for the spatial separation of the components. For example, the low kT gas could be spatially localized on a CD galaxy in the cluster while the hot gas would then be uniformly distributed. Alternatively the two components could be mixed in a situation analogous to the "swiss cheese" model of the interstellar medium.

Assuming pressure balance holds in the cluster gas one has a ratio of volumes of the two components in the Centaurus cluster of $V_{Low}/V_{High} \sim .4$ or a scale length ratio of ~ 1.3 and in the A1060 cluster $V_1/V_2 \sim .1$ and a scale length ratio of ~ 3. Given that a single galaxy would occupy $\leq .001$ of the core volume of a typical cluster one concludes that the gas must be dispersed in a "swiss cheese" type model.

This has strong implications for the X-ray appearance of the cluster to an imaging telescope. The low kT gas, because of its ~ 4 times higher density, will have ~ 16 times the surface brightness of the hot gas. However, because the two components have roughly equal volumes the cluster will look "spotty" if the number of blobs of gas in the cluster is less than or equal to the number of galaxies in the cluster. In the Centaurus clusters the surface area of the high and low surface brightness regions would be roughly equal while in A1060 most o f the area will be taken up by low surface brightness gas and the cluster might appear to have bright spots. Actual measurements of the surface brightness will help to confirm the assumption of pressure equilibrium in these clusters.

Alternatively one can assume that the two regions are not intermixed and that the "hot" component is at the center of the cluster surrounded by the larger "cold" component. Recent results from the HEAO A-3 modulation collimator (Schwartz et al. 1979) report that $\sim 1/5$ of the flux from Centaurus comes from a region smaller than 35.0 kpc centered on NGC 4696. Equating this flux with our "hot" component, which has $\sim 1/5$ of the total flux of the cluster one derives a mean density of 6×10^{-4} cm^{-3} for the hot component. Assuming pressure equilibrium the cool gas has $\bar{n}_c \sim 2.4 \times 10^{-3}$ and a characteristic size of 50 kpc. Again actual measurements of the surface brightness combined with our spectral data will help resolve the ambiguity.

Comparing the velocity dispersions and central galaxy densities for Centaurus, A1060, Virgo, and A2147 as listed in Mushotzky et al. 1978, we see some evidence that it is the lower temperature component that correlates well with the depth of a cluster's gravitational potential. If the higher energy component is thermal, this would imply the existence of a heating mechanism for that part of the gas with an origin other than movement into the potential well of the cluster, since the depth of the well appears insufficient to produce the higher temperature. This also would imply that this gas is not bound to the cluster and must be escaping in the form of a cluster wind (Yahil and Ostriker 1973). Finding a good correlation between some temperature component and gravitational potential (as measured by velocity dispersion or central galaxy density) improves the correlations shown in Mushotzky et al. (see also Smith et al. 1979). The possibility that the higher energy component in these clusters is of nonthermal origin is discussed below.

C. Extended Halos

Because of the closeness of the Centaurus and the A1060 clusters measurements of the relative flux in the 3 x 3 vs. 3 x 1.5^{0} fields of view set a strong limit on the physical size of these objects. Following the analysis of Nulsen et al. 1979 we find a scale size for a King model of $\leq$ .6 Mpc in Centaurus and $\leq$ .8 Mpc in A1060. These values are considerably less then the "typical" halo values found by Forman et al. 1978. These results agree with those from a large sample of clusters studied by Pravdo et al. 1979 and Nulsen et al. 1979.

D. Inverse Compton Emission

The discovery of a two component nature to the X-ray continuum raises the possibility that the second component could be non-thermal. This possibility, that some of the X-ray flux could be inverse-Compton in origin, has been discussed in detail by Harris and Romanishin (1974). If it is, the Fe abundance in the low temperature gas is quite high, (see Section VA) ($\sim$ 1.5 solar) but this result does not rule out possible Compton emission.

Both the Centaurus and A1060 clusters have low frequency radio emission (Erickson, Viner and Matthew 1978) with power law energy indices of 1.13 and 1.0 respectively. These slopes compare to the $\alpha \sim 1.1 \pm .2$ and $1.2 \pm .3$ for the hard X-ray component, this rough agreement makes the possibility of Compton emission reasonable.

If the hard X-ray flux is inverse-Compton we can calculate the magnetic field in the cluster of $\sim 3 \times 10^{-8}$ gauss in Centaurus and $\sim 1.5 \times 10^{-8}$ gauss in A1060 obtained from the ratio of X-ray and radio fluxes. This is to be compared to expected magnetic field strengths of $\sim 10^{-6} - 10^{-7}$ in clusters of galaxies from equipartition arguments. Thus it is indeed possible that we have detected inverse Compton X-ray emission in these clusters. This situation is only possible when the thermal component is very low in luminosity compared to that of most other clusters and the magnetic field is also much lower then expected for equipartion. Observations at higher energies will be able to tell if the second component is thermal or inverse Compton.

ACKNOWLEDGMENTS

RJM gratefully acknowledges the hospitality of Elihu Boldt and the Goddard Space Flight Center X-ray Astronomy Group. Financial support for RJM came from an S.R.C. research grant. We thank Dr. Andy Fabian for useful suggestions, and Dr. B.W. Smith for help with the theoretical interpretation.

REFERENCES

Abell, G. 1958, Ap. J. Suppl. 3, 211.

Erickson, W.C., Matthews, T.A., and Viner, M.R. 1978, Ap. J. 222, 761.

Forman, W., Jones, C., Murray, S., and Giacconi, R. 1978, Ap. J. (Letters) 225, L1.

Gursky, H., Kellogg, E., Leong, C., Tananbaum, H., and Giacconi, R. 1971, Ap. J. (Letters) 167, L81.

Harris, D.E. and Romanishin, W. 1974, Ap. J. 188, 209.

Ives, J.C. and Sanford, P.W. 1976, M.N.R.A.S. 176, 13.

Jones, C. and Forman, W. 1978, Ap. J. 224, 1.

Kellogg, E. and Murray, S. 1974, Ap. J. (Letters) 193, L57.

Kellogg, E., Baldwin, J.R. and Koch, D. 1975, Ap. J. 199, 299.

Mitchell, R.J., Dickens, R.J., Bonell, J.L. and Culhane, J.L. 1979, M.N.R.A.S., in press.

Mitchell, R.J., Charles, P.A., Culhane, J.L., Davison, P.J.N., and Fabian, A.C. 1975, Ap. J. 200, L5.

Mitchell, R. and Culhane, L. 1977, M.N.R.A.S. 178, 75.

Mushotzky, R., Serlemitsos, P.J., Smith, B.W., Boldt, E.A., and Holt, S.S. 1978, Ap. J. 225, 21.

Nulsen, P., Fabian, A., Mushotzky, R., Boldt, E., Holt, S., Marshall, F.J., and Serlemitsos, P.J. 1979, M.N.R.A.S., in press.

Pravdo, S., Boldt, E., Marshall, F., McKee, J., Mushotzky, R.E., Smith, B.W., and Reichert, G. 1979, Ap. J., in press.

Raymond, J. and Smith, B.W. 1977, Ap. J. Suppl. 35, 419.

Rothschild, R.E. et al. 1979, Space Science Inst., in press.

Schwartz, J., Schwartz, D.A., Johnston, M.D., Doxsey, R.E. 1979, B.A.A.S. 11, 460.

Smith, B.W., Mushotzky, R.F. and Serlemitsos, P.J. 1979, Ap. J. 227, 37.

Yahil, A. and Ostriker, J.P. 1973, Ap. J. 185, 787.

TABLE 1A

MODEL	DETECTOR	kT (KeV)	LINE STRENGTH (ph/cm^2 sec)	PEAK ENERGY (keV)	χ^2 MIN
Isothermal	MED	3.68			261
Isothermal	HED 3	4.65			142
Isothermal & Iron Line	MED	3.15	$9.3\ 10^{-4}$	6.86	70
Isothermal & Iron Line	HED 3	4.22	$5.1\ 10^{-4}$	6.73	68

TABLE 1B

MODEL	DETECTOR	kT_1	kT_2	6.7 keV BLEND LINE STRENGTH	6.7 keV BLEND PEAK ENERGY	7.9 keV BLEND LINE STRENGTH	7.9 keV BLEND PEAK ENERGY	χ^2_{min}
2 Isothermals + 1 Line	MED	1.99	6.49	$8.2\ 10^{-4}$	6.81			41
2 Isothermals + 1 Line	HED 3	2.83	8.74	$5.93\ 10^{-4}$	6.69			60
1 Isothermal + 2 Lines	MED	3.00		$8.3\ 10^{-4}$	6.73	$3.9\ 10^{-4}$	8.19	41
1 Isothermal + 2 Lines	HED 3	4.05		$5.36\ 10^{-4}$	6.64	$2.09\ 10^{-4}$	8.06	60

TABLE 1C

MODEL	DETECTOR	kT_1	kT_2	6.7 keV Blend LINE STRENGTH	6.7 keV Blend PEAK ENERGY	7.9 keV Blend LINE STRENGTH	7.9 keV Blend PEAK ENERGY	RATIO 7.9/6.7 LINE FLUX	χ^2_{min}
2 Isothermals + 2 Lines	MED	2.31	7.20	$8.45\ 10^{-4}$	6.70	$2.74\ 10^{-4}$	7.96	0.32	23.6
2 Isothermals	HED 3	2.32	8.81	$6.55\ 10^{-4}$	6.57	$2.66\ 10^{-4}$	7.90	0.406	46.8

TABLE 1D

MODEL	DETECTOR	kT	α	6.7 keV Blend LINE STRENGTH	6.7 keV Blend PEAK ENERGY	7.9 keV Blend LINE STRENGTH	7.9 keV Blend PEAK ENERGY	RATIO 7.9/6.7 LINE FLUX	χ^2_{min}
1 Isothermal + 1 Power Law + 2 Lines	MED	2.68	2.06	$8.6\ 10^{-4}$	6.69	$2.8\ 10^{-4}$	7.97	0.33	30
1 Isothermal + 1 Power Law + 2 Lines	HED 3	3.41	2.29	$6.77\ 10^{-4}$	6.58	$2.6\ 10^{-4}$	7.95	0.27	51

TABLE 2

MODEL	DETECTOR	kT_1	kT_2	α	LINE STRENGTH	PEAK ENERGY	χ^2_{min}
1 Isothermal	MED	3.15					91
1 Isothermal	HED 3	3.83					107
1 Isothermal + 1 Line	MED	2.80			$3.4\ 10^{-4}$	7.07	65
1 Isothermal + 1 Line	HED 3	3.27			$3.4\ 10^{-4}$	6.41	83
2 Isothermals + 1 Line	MED	1.80	14.4		$2.37\ 10^{-4}$	6.95	50
2 Isothermals + 1 Line	HED 3	2.24	11.9		$3.5\ 10^{-4}$	6.36	76
1 Isothermal + 1 Power Law + 1 Line	MED	1.89		2.05	$4.40\ 10^{-4}$	6.96	50
1 Isothermal + 1 Power Law + 1 Line	HED 3	2.39		2.42	$3.5\ 10^{-4}$	6.37	76

TABLE 3

EMISSION INTEGRAL FOR CLUSTERS

	Low kT	High kT
Cen	$\sim 1.3 \times 10^{67}$	$\sim 3.2 \times 10^{66}$
A1060	$\sim 5.3 \times 10^{66}$	$\sim 2.2 \times 10^{66}$

FIGURE CAPTIONS

Figure 1 - The MED data for the Centaurus cluster.

1a - The fit to a single exponential + 6.7 keV iron feature.

1b - The fit to a 2-exponentials + 2-lines model. Dashed and dotted histograms show the contributions from the individual continua.

1c - The resulting photon spectrum after folding (b) through the detector resolution and response functions. Higher-energy channels have been combined in order to avoid cluttering the figure.

Figure 2 - The HED 3 data for the Centaurus cluster. The captions (a), (b), and (c) for Figure 1 also apply here.

Figure 3 - χ^2 versus line strength for the 6.7 and 7.9 keV lines seen in the Centaurus cluster spectrum showing ranges of acceptable values derived from the MED and HED 3 data.

Figure 4 - χ^2 contours showing acceptable temperatures for the two thermal components in a 2-continuum + 2-line model fitted to the MED and HED 3 Centaurus data. Contours are plotted at the χ^2_{min} + 2 and χ^2_{min} + 5 levels. Note that the MED data excludes temperatures above 2.9 keV for the low temperature component while the HED 3 data excludes temperatures below 4.5 keV for the high temperature component. Also note that a good fit to both data sets can be achieved for low and high temperatures of around 2.5 keV and 7 keV respectively.

Figure 5 - The HEAO-A2 90% confidence error box for the X-ray source believed to be associated with the cluster of galaxies A 1060. The cluster center and 2A and 4U error boxes are also indicated.

Figure 6 - The MED data for the A1060 cluster. Captions for 1(a), (b), and (c) apply except that no 7.9 keV line has been included in the spectral fits shown in 6 (b) or (c).

Figure 7 - The HED 3 data for the A1060 cluster. 7(a), (b) and (c) are complementary to the corresponding figures in 6.

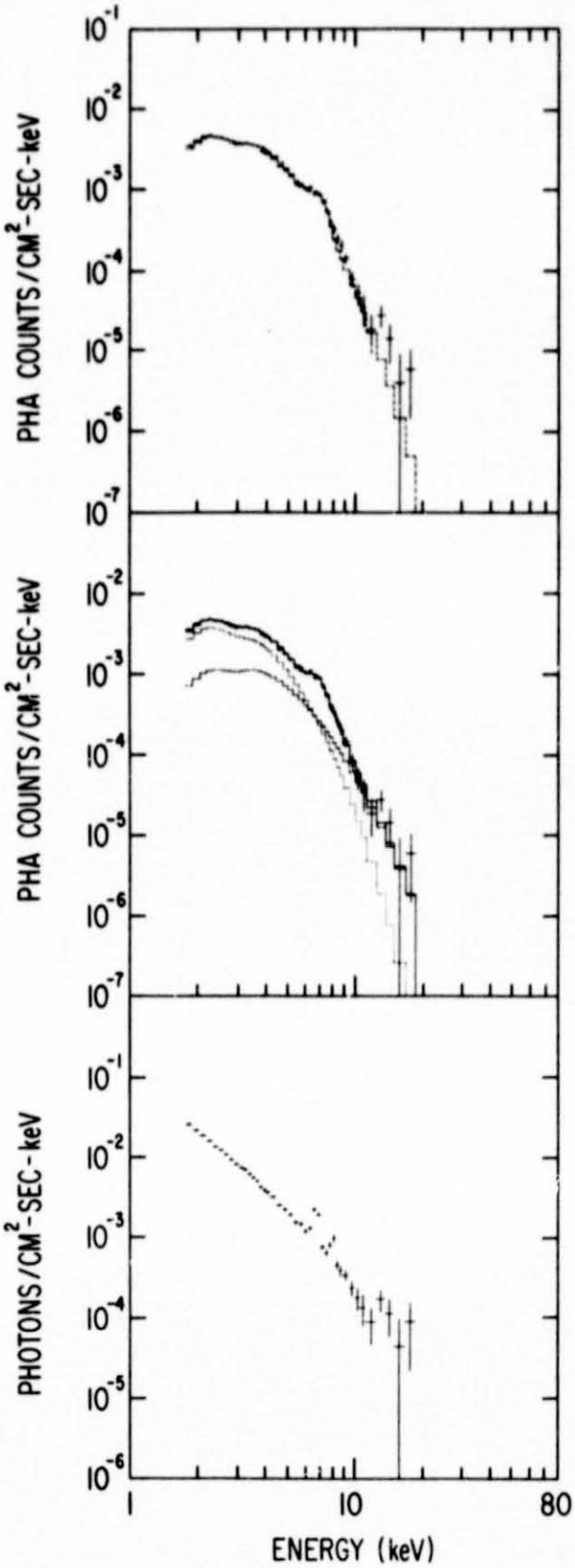
PHA COUNTS/CM²-SEC-keV
PHA COUNTS/CM²-SEC-keV
PHOTONS/CM²-SEC-keV
10⁻¹
10⁻²
10⁻³
10⁻⁴
10⁻⁵
10⁻⁶
10⁻⁷
1
10
80
ENERGY (keV)

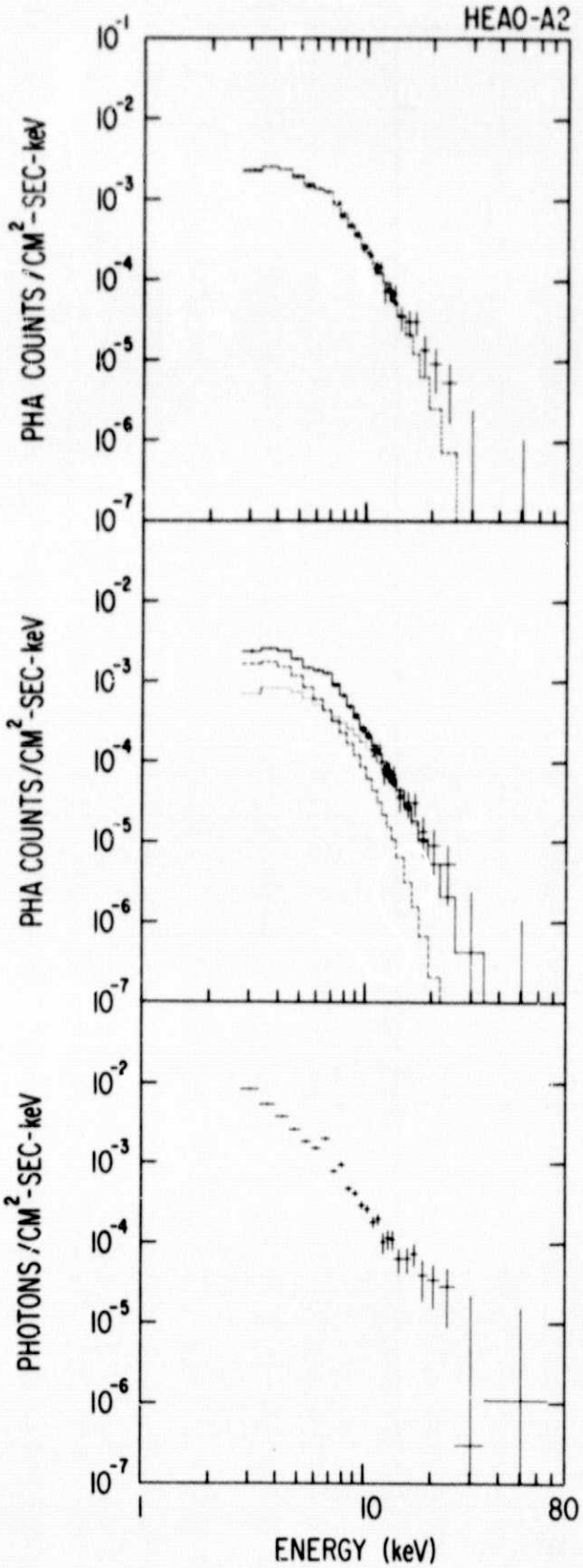
HEAO-A2
PHA COUNTS /CM²-SEC-keV
PHA COUNTS/CM²-SEC-keV
PHOTONS /CM²-SEC-keV
10⁻¹
10⁻²
10⁻³
10⁻⁴
10⁻⁵
10⁻⁶
10⁻⁷
1
10
80
ENERGY (keV)

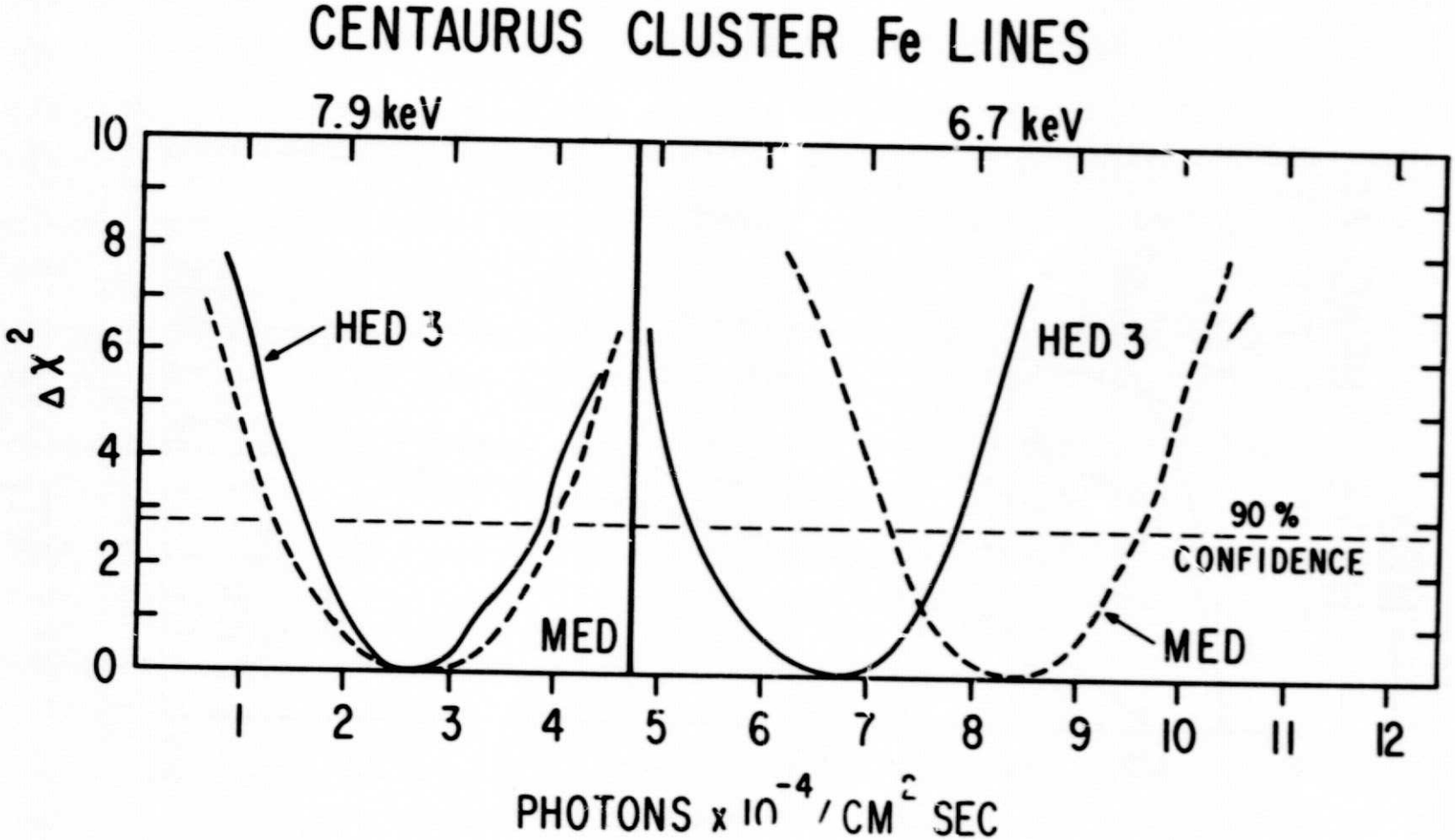
CENTAURUS CLUSTER Fe LINES
7.9 keV
6.7 keV
10
8
6
4
2
0
$\Delta\chi^2$
HED 3
HED 3
MED
MED
90 %
CONFIDENCE
1
2
3
4
5
6
7
8
9
10
11
12
PHOTONS x 10^{-4} / CM^2 SEC

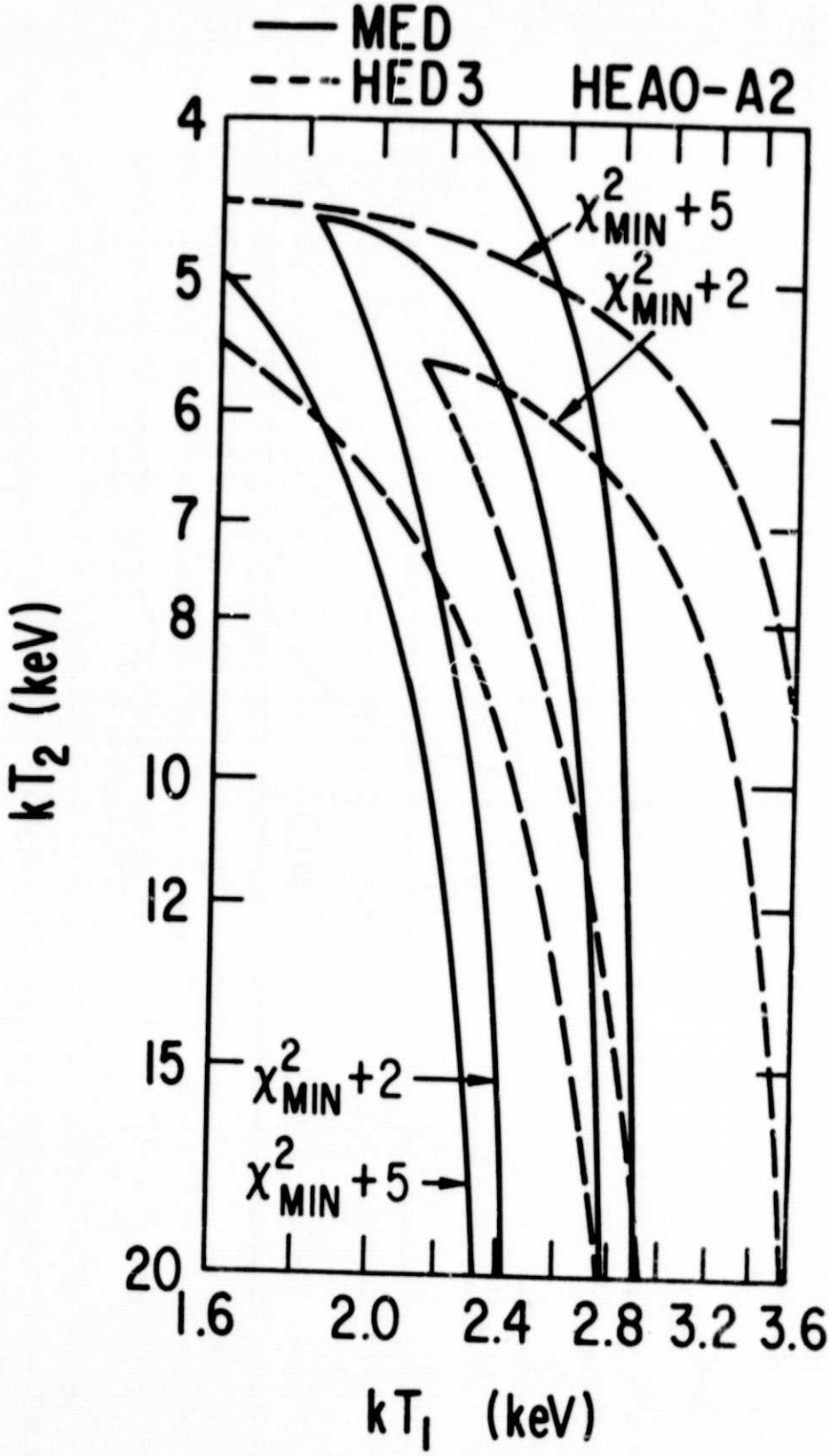
MED
HED3
HEAO-A2
$\chi^2_{MIN}+5$
$\chi^2_{MIN}+2$
$\chi^2_{MIN}+2$
$\chi^2_{MIN}+5$
kT_2 (keV)
kT_1 (keV)
4
5
6
7
8
10
12
15
20
1.6
2.0
2.4
2.8
3.2
3.6

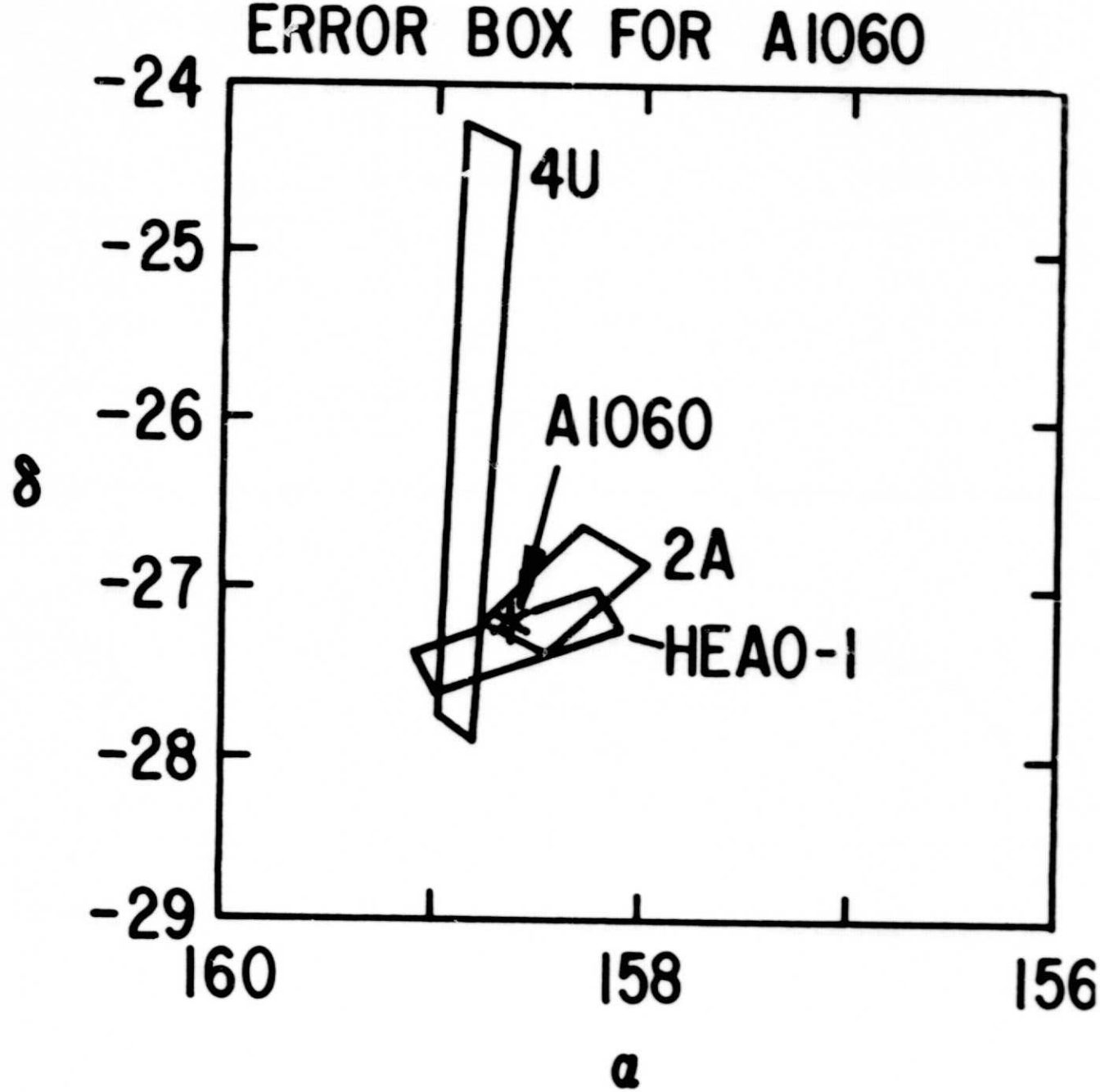
ERROR BOX FOR A1060
-24
-25
-26
-27
-28
-29
δ
4U
A1060
2A
HEAO-1
160
158
156
α

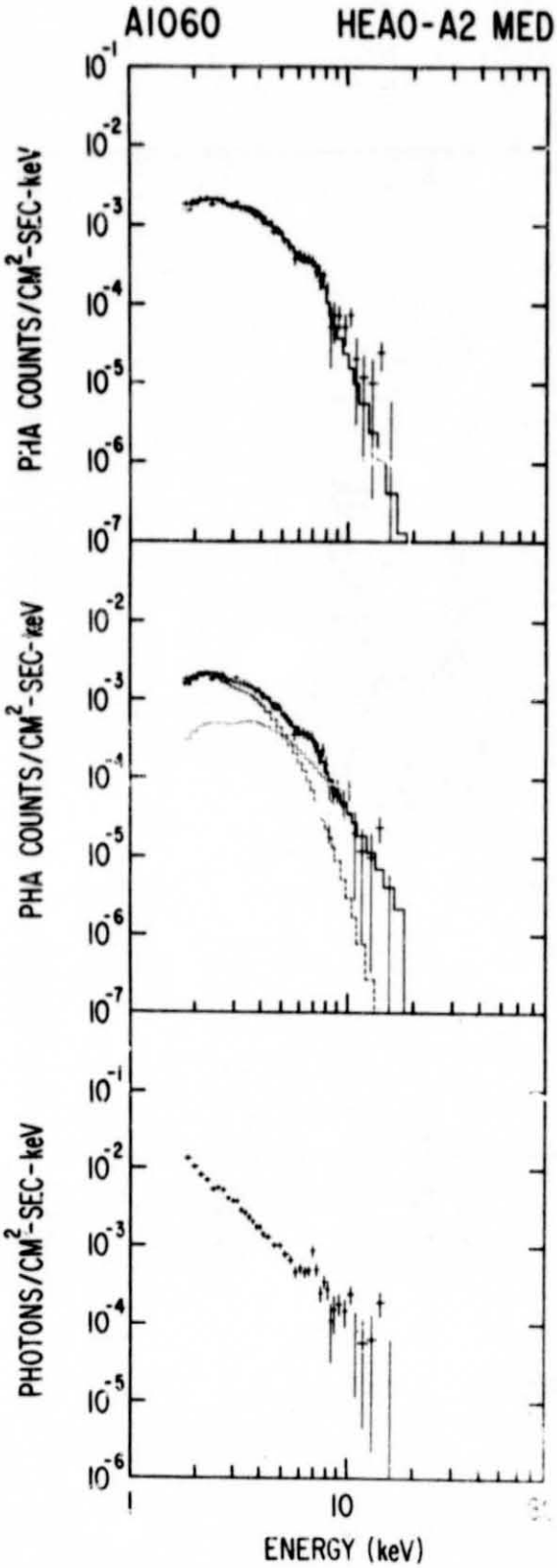
A1060
HEAO-A2 MED
PHA COUNTS/CM²-SEC-keV
PHA COUNTS/CM²-SEC-keV
PHOTONS/CM²-SEC-keV
10⁻¹
10⁻²
10⁻³
10⁻⁴
10⁻⁵
10⁻⁶
10⁻⁷
1
10
ENERGY (keV)

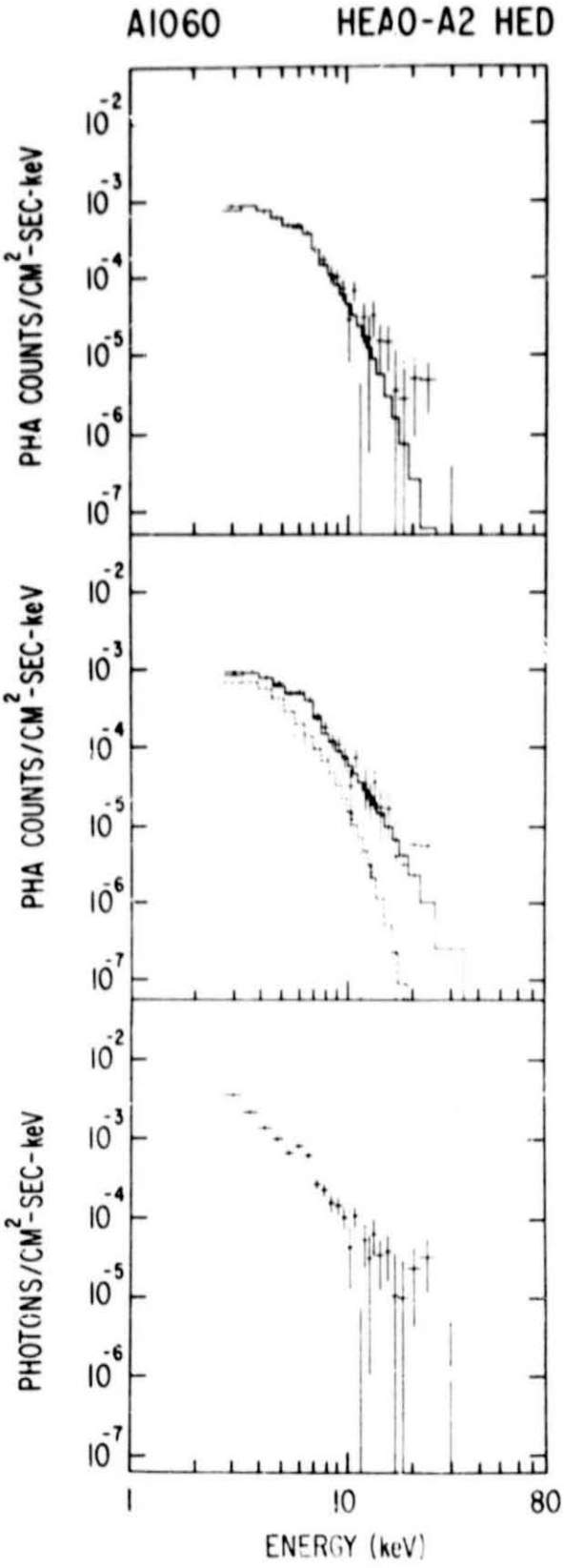
A1060
HEAO-A2 HED
PHA COUNTS/CM²-SEC-keV
PHA COUNTS/CM²-SEC-keV
PHOTONS/CM²-SEC-keV
10⁻²
10⁻³
10⁻⁴
10⁻⁵
10⁻⁶
10⁻⁷
1
10
80
ENERGY (keV)